SUPPLEMENTARY INFORMATION

1. ASTROMETRIC MEASUREMENTS AND PREDICTION OF THE SHADOW PATH ON EARTH.

For Makemake there are typically 3 potential occultations per year[13], but most of them are too challenging or impossible to observe: some of them involve too faint stars, others take place at too high airmasses or in daylight, or in remote areas of the world where deploying a network of telescopes is too difficult. Besides, the initial shadow path predictions have typical errors of a few thousand km so updates are necessary. Thus, potentially good occultations are rare. This situation may change in the future when high accuracy astrometric data from the GAIA space mission become available, but currently most occultations are difficult to observe and uncertain. The occultation of the faint star NOMAD 1181-0235723 by Makemake was initially predicted in 2010 by following the methods described in a recent work[13]. The star magnitude was 18.24 and 18.55 in the r and g bands respectively, according to the 11th release of the SDSS photometric catalog. The initial occultation prediction was not favorable: it indicated that Makemake's shadow would miss the Earth by about 1000 km on April 23rd at approximately 1:30 UT. Astrometric refinement of the star's and Makemake's positions from CCD images obtained days prior to the occultation showed that the shadow path of the occultation would pass over South America (Fig. S1). A total of 108 astrometric measurements were obtained during 5 nights from images acquired at the f/3 0.77m telescope of La Hita observatory (Spain) in the period April 8th to April 12th 2011. The telescope is equipped with a 4kx4k camera that provided a field of view of 48.1'x 48.1' with a 0.705 arcsec/pixel scale. The observing technique and reductions were identical to those used to obtain high accuracy astrometry of Orcus[28]. The J2000 coordinates of the star determined from the observations were:

Right Ascension (RA): 12h 36m 11.4018s

Declination (Dec): +28° 11' 10.448''

The dispersion in the astrometry of the star was 0.13 arcsec in RA and 0.06 arcsec in Dec. For comparison, Makemake's angular diameter is 0.038 arcsec. From the Makemake astrometry, offsets of Makemake relative to JPL ephemerides JPL#24 were obtained. They were applied to the star coordinates and the shadow path prediction was computed using the Makemake JPL orbital elements for the time of the occultation. The prediction turned out to be off by approximately -3 minutes of time compared to the occultation observations and the shadow path was approximately 300 km south of the final path, shown in Fig. S1.

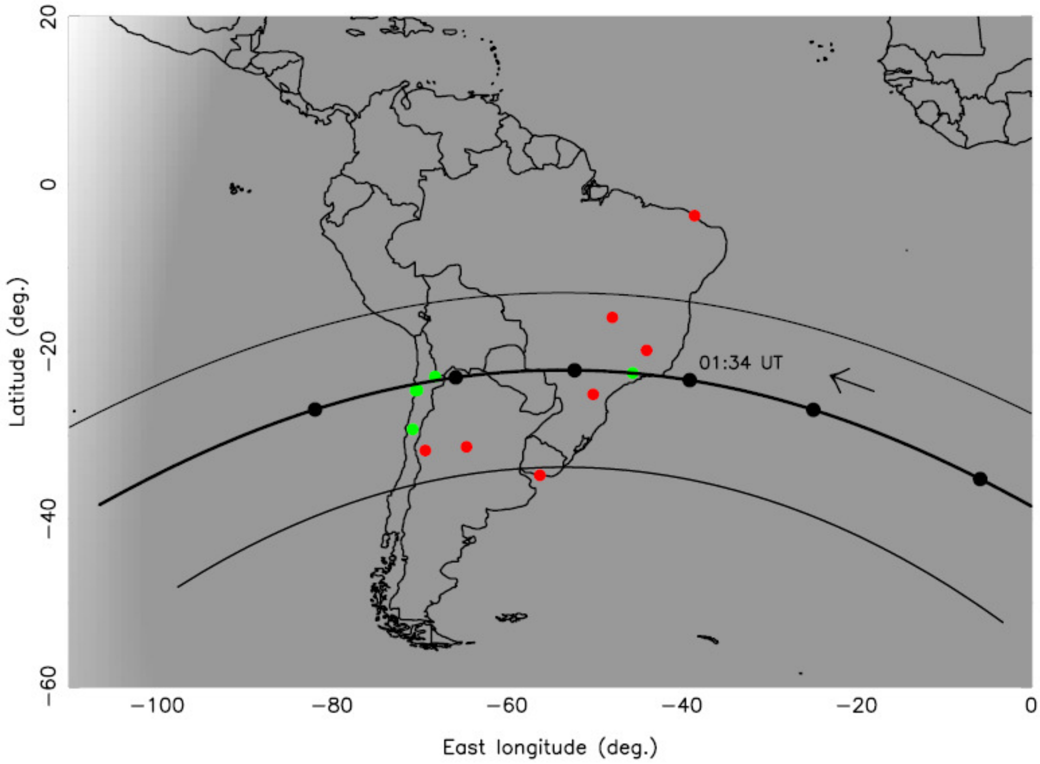

Fig. S1. Makemake's shadow path on Earth based on the occultation results. The width of the shadow path corresponds to an assumed diameter of 1,430 km. The dots on the centreline are plotted every minute. A reference dot is indicated at 01:34 UT, April 23, 2011, and the arrow indicates the direction of motion of the shadow. The locations listed in Tables S1 are plotted in green for the sites where the occultation was detected, and in red for stations with clouds or technical problems. The green dot on the right corresponds to Pico dos Dias observatory where the event was observed about 100 s before the Chile stations.

2. LIST OF ALL THE TELESCOPES THAT OBSERVED OR ATTEMPTED TO OBSERVE THE OCCULTATION.

Table S1. Sites and telescopes that observed the event. In the comments column we include the average signal to noise ratio (SNR) per data point, outside the occultation, for those sites that had a positive result. Note that the integration times were different for each telescope, which explains the various SNR values reached. The synthetic aperture radii used were 1.05, 2.6, 0.6, 2.9, 3.2, 2.4, and 4.0 arcsecs for NTT, TRAPPIST, VLT, Armazones, S. Pedro de Atacama Harlingten, S. Pedro de Atacama ASH2 and Pico dos Dias, respectively. These radii typically corresponded to 2 pixels.

Site	**Telescope**	**Longitude** **Latitude** **Height**	**Results**	**Comment**
La Silla	3.5m NTT+ULTRACAM	70°44'01.5"W, 29°15'31.8"S, 2345.4 m	Positive	SNR=15
La Silla	0.6m TRAPPIST	70°44'21.7"W, 29°15'16.6"S, 2317.7 m	Positive	SNR=22
Paranal	8m VLT+ISAAC	70°24'09.9"W, 24°37'30.3"S, 2635m	Positive	SNR=15
Paranal	8m VLT+FORS2	70°24'09.9"W, 24°37'30.3"S, 2635 m	Negative	Image acquisition started too late
Armazones	0.84m OCA	70°11'46.4"W, 24°35'51.9"S, 2705.7 m	Positive	SNR=25
San Pedro de Atacama	0.5m Harlingten	68°10'47.0"W, 22°57'12.2"S, 2305 m	Positive	SNR=21
San Pedro de Atacama	0.4m ASH2	68°10'47.0"W, 22°57'12.2"S, 2305 m	Positive	SNR=23
Pico dos Dias	0.6m Carl Zeiss	45°34'57.5"W, 22°32'07.8"S, 1810 m	Positive	SNR=15
Pico dos Dias	0.6m Boller & Chivens	45°34'57.5"W, 22°32'07.8"S,	Negative	Instrument problems

		1810 m		
Cerro Burek	0.6m Helen Sawyer Hogg	69°18'25.9"W, 31°47'14.5"S, 2591 m	Negative	Technical problems
Los Molinos	0.45m	56°11'24.6"W, 34°45'19.3S, 80m	Negative	Clouds
Tanti – Córdoba	0.36m	64º35'34.41"W, 31º21'24.58"S, 862 m	Negative	Technical problems
Fortaleza	0.3m	38º30'27"W, 3º44'18"S, 38 m	Negative	Clouds
CEAMIG-REA	0.3m	43º59'51"W, 19º49'49"S, 825 m	Negative	Clouds
Brasilia	0.25m	47º54'40.6"W, 15º53'29.1"S, 1072 m	Negative	Clouds
Ponta Grossa	0.4m	50º05'56"W, 25º05'22"S, 909 m	Negative	Clouds

3. CHORDS AND THEIR ANALYSIS.

Square well models were fit to the occultation light curves by minimizing a χ^2 defined as:

$$\chi^2 = \sum_1^N \frac{(F_{\mathrm{mod},i} - F_i)^2}{\sigma_i^2} \tag{1}$$

where $F_{mod,i}$ is the modeled flux at image number *i*, F_i is the observed flux at image number *i* and σ_i are the measurement errors, and N is the number of images. The model took into account diffraction, bandwidth, stellar angular diameter and integration time. The effect of time errors as small as 10 ms and 1 ms were entirely negligible compared to the errors in the fluxes (keeping in mind that the ratios of integration times to time uncertainties were always larger than 1,000) so they were not taken into account. The main parameters of the model are the depth of the square well and the disappearance time as well as the reappearance time of the occultation. The uncertainties in the retrieved parameters were obtained from a grid search in the parameter space. Acceptable values were those that gave a χ^2 within $\chi^2_{\min}$ and $\chi^2_{\min}+1$

From the fitted times at the different sites, one can generate chords in the projected plane of the sky, which represent the motion (in milli-arcsecs) of the star relative to the TNO as seen from the different sites. One can fit a shape to the extremities of the chords. We fitted elliptical and circular shapes by minimizing a χ^2 function defined as follows:

$$\chi^2 = \sum_1^N \frac{(f_{i,obs} - f_c)^2}{a^2 \sigma_{i,r}^2} + \frac{(g_{i,obs} - g_c)^2}{b^2 \sigma_{i,r}^2} \tag{2}$$

where f_i and g_i are the positions of the star in the plane of the sky relative to Makemake as seen from each observing site at ingress and egress times, *a* and *b* are the semiaxes of the ellipse (in a circular fit both axes are equal). In this case $\sigma_{i,r}$ are the errors of the extremities, which were derived from the errors in the retrieved ingress and egress times and N is the number of extremities. Last, f_c and g_c are the centers of the ellipse in the f,g plane. The best fit was obtained by means of a Marquardt-Levenberg minimization routine. The retrieved a,b parameters in milli-arcsecs (mas) were translated into length in km by using the known distance of Makemake from Earth, according to its ephemerides (which gave 37.35 km/mas). The velocity of Makemake with respect to the star was 22.12 km/s. The 1σ uncertainties in the parameters were obtained from the Marquardt-Levenberg fitting routine.

4. GEOMETRIC ALBEDO COMPUTATIONS.

Once the apparent area (A) of Makemake was obtained from the limb fit to the occultation chords, we used the expression that relates the geometric albedo (p_V), absolute magnitude (H_{obj}), magnitude of the sun (H_{sun}) and the projected area of a solar system body:

$$p_v = \frac{10^{0.4(H_{sun} - H_{obj})}}{(A/\pi)} \tag{3}$$

to derive p_V. We should take into account that the area A in the above equation is expressed in square astronomical units (AU), with 1 AU = 149598000 km. We used an absolute magnitude H_V = 0.091±0.015 from ref. 17 and the usual solar magnitude $H_{sun,V}$ = -26.74. The resulting geometric albedo in the V band is 0.77±0.03 for an object with projected axes a'=1,502±45 km, and b'=1,430±9 km. The main uncertainty in the albedo comes from the error in the projected area

($\pi a'b'$). The geometric albedo in the R band was obtained from the V-R color of Makemake, implying that H_R = -0.395±0.02. Using that result for H_R and a value of $H_{sun,R}$ = -27.08 we obtained the following geometric albedo in the red p_R = 0.90±0.02.

5. THERMAL MODELS OF MAKEMAKE AND EQUILIBRIUM TEMPERATURES.

The equilibrium temperature of an airless spherical body can be computed by using a standard thermal model

$$T_{eq}^4 = \frac{F_{sun}(1 - Alb)}{\sigma\varepsilon\eta\zeta\ r^2} \tag{4}$$

where *Alb* is the bond albedo, F_{sun} = 1,360 W m^{-2} is the solar constant (Solar Flux at 1 AU), σ = 5.67x10^{-8} W m^{-2} K^{-4} is the Stefan-Boltzmann constant, and the emissivity (ϵ) accounts for the deviation of pure blackbody emission (usually assumed to be 0.9 based on asteroid studies). The beaming parameter (η) takes into account some anisotropic emission effects as a result of surface roughness and thermal inertia and is usually thought to be around 1.2 for TNOs (ref. 5). The variable r is the heliocentric distance of the body in astronomical units and ζ is a parameter that takes the value of π if the object is a fast rotator or 2 if it is a slow rotator. If we want to know the temperature at the subsolar point, this parameter must be set to 1. On the other hand Alb = $p_V q$, where p_V is the geometric albedo of the object, and q is the phase integral. This parameter is probably close to 0.75 for Makemake: There is an empirical relation between geometric albedo and phase integral based on TNO observations[29] and also based on observations of the satellites of the outer planets[30]. From those papers almost identical predictions for the phase integral of Makemake are obtained, around 0.75.

Using a value of 0.77 for the geometric albedo, a phase integral of 0.75, an emissivity of 0.9, a beaming parameter of 1.2, and the distance at which the occultation by Makemake took place (52.21 AU) we get an equilibrium temperature for Makemake of only 36 K and 32 K (for the slow rotator and fast rotator cases respectively). However, we know that 0.77 is the average geometric albedo, and in fact we know that Makemake must have a dark terrain to account for the Spitzer and Herschel measurements[5,6,23]. The dark terrain must have a geometric albedo of 0.12 or lower. Using the thermal model with this input for the geometric albedo, we get a temperature of 44 K for the slow rotator case and 40 K for the fast rotator case. The result is 52 K at the subsolar point or even higher if we use a lower than 0.12 geometric albedo. This temperature is high enough for substantial nitrogen and even methane ice sublimation.

6. LIMITS ON A GLOBAL ATMOSPHERE FROM THE NTT AND VLT INGRESS AND EGRESS PROFILES.

Makemake has an icy surface with CH_4 ice (e.g. ref. 4) and perhaps N_2 ice. An atmosphere may then be maintained through vapour pressure equilibrium between the ice and its gaseous counterpart. The ice temperature T_{surf} controls the atmospheric surface pressure P_{surf} through sublimation processes, and for pure ices, we may use laboratory measurements to relate T_{surf} and P_{surf} (ref. 25). More complicated laws apply when the ices are mixed but we use here the approximation that a pure ice (either CH_4 or N_2) is in vapour equilibrium with its gaseous counterpart. The occultation probes Makemake's limb, where the temperature possibly varies from 35 K down to 10 K (see Fig. S4 where we show an example). We examine the possibilities of a pure CH_4 atmosphere, an N_2 atmosphere with a small amount of CH_4, and a pure N_2 atmosphere.

6.1 Pure CH_4 atmosphere

A pure CH_4 atmosphere should start at the surface with a temperature between 10 and 35 K, but near-IR heating should increase this temperature within a few kilometers, to reach an isothermal branch, as observed in Pluto's atmosphere[31,32]. Considering that Pluto's upper atmosphere is at about 106 K, and that the solar insolation at Makemake is reduced by a factor of about 2.8 with respect to Pluto, a rough estimation of a CH_4 atmosphere temperature at altitude is about 100 K. For the thermal gradient near the surface, we adopt a value of 17 K km^{-1}. This high value is typical of what is expected for methane-rich atmospheres[31,32].

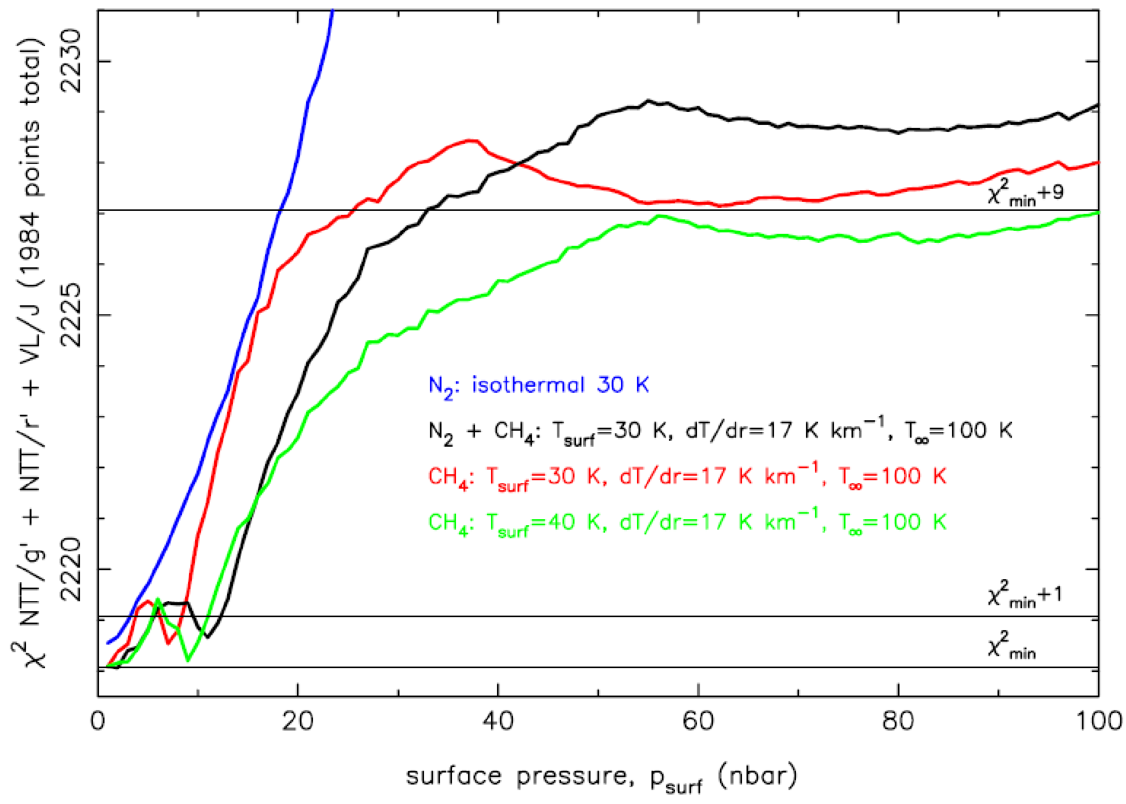

Fig. S2: χ^2 values obtained by varying the surface pressure P_{surf} of the four CH_4 and N_2 atmospheres described in the text. The surface temperature, temperature gradient and the upper level temperature are indicated for each of the three curves. The red line corresponds to a pure CH_4 atmosphere, the blue line is for a pure N_2 atmosphere and the black line corresponds to an N_2 atmosphere with some CH_4 to generate a temperature gradient. The green line is the same as the red line but for a higher surface temperature. Note that most of the constraints come from the NTT data since the VLT data have a lower time resolution.

A ray-tracing program provides the expected ingress and egress occultation light curves caused by such an atmosphere, keeping the surface pressure P_{surf} as a free parameter. We have adjusted this model to the NTT data points (g' and r' channel), as well as to the VLT observations (J-band). Only the NTT and VLT data have been used because they present the highest signal to noise and have good enough time resolution. A standard χ^2 analysis provides the goodness of the fits. We used N = 1984 data points in total, obtaining a minimum χ^2 value of $\chi^2_{\min}$= 2218 for P_{surf} = 0 nbar, which corresponds to a value of χ^2_{pdf} = 1.1 per degree of freedom (red curve in Fig. S2). Thus, the data are consistent with a complete absence of atmosphere, at least at the points of the limb probed by the occultation. The increase of χ^2 to $\chi^2_{\min}$ + 1 actually provides a 1σ upper limit of about 8 nbar for the surface pressure of the putative CH_4 atmosphere considered here. If one relaxes the 1σ limit to a 3σ level (increase of χ^2 to $\chi^2_{\min}$ + 9), we obtain a limit of about 25 nbar. Taking a surface temperature of 40 K, instead of 30 K, and everything equal besides, we obtain a 1σ limit of 11 nbar for P_{surf}, and no stringent 3σ limit up to values of 100 nbar or more (Fig. S2). This is because the deep, denser, part of the atmosphere causes a shallow bottom in the occultation light curve that becomes undistinguishable from the noise in the data (see Fig. 3).

In conclusion, a 1σ level upper limit of about 10 nbar can be placed for the surface pressure of a CH_4 atmosphere, but the data could accommodate denser atmospheres (up to 100 nbar or more) if a 3σ level is considered, or if surface temperatures larger than 30 K are considered. This said, 10 nbar corresponds the equilibrium vapour pressure of CH_4 for a temperature of about 40 K (ref. 25). This is larger than the temperature expected along Makemake's limb, and is thus consistent with our non-detection of a global CH_4 atmosphere at the 10 nbar limit.

6.2 N_2 atmosphere

A putative nitrogen atmosphere is likely to be mixed with CH_4, considering the detection of the latter species on Makemake's surface (e.g. ref. 4). Thus, the same general thermal structure is expected as for CH_4, namely an atmosphere starting from a cold surface, and then reaching a warmer isothermal branch after a few kilometers. In that case, an upper limit of P_{surf} = 12 nbar can be derived at the 1σ level, comparable to the pure CH_4 atmosphere case (black curve in Fig. S2), and P_{surf} of about 35 nbar at the 3σ level. The P_{surf} = 12 nbar value would correspond to a vapour pressure equilibrium with a N_2 surface ice at 29 K, consistent with our starting assumption of T_{surf} = 30 K. The possibility still exists, however, that Makemake's atmosphere would be essentially pure N_2, since this gas is much more volatile than CH_4 by about 5 orders of magnitude. In that case, a 1σ upper limit for P_{surf} is about 4 nbar, and the corresponding 3σ limit would be about 20 nbar (blue curve in Fig. S2).

In conclusion, the various atmospheric models considered here place 1σ level upper limits of 4-12 nbar for the surface pressure, while less stringents upper limits in the range 20-100 nbar are obtained at the 3σ level. We note also that we have used a large value of the thermal gradient near the surface (17 K km^{-1}). Lower values of that gradient would provide more stringent limits on P_{surf}. We have actually examined here the less favorable cases, where a thin inversion layer close to the surface remains unnoticed due to the shape of the light curve and the noise in the data (see the dash-dotted curve in Fig. 3)

7. DISCUSSION ON A LOCAL ATMOSPHERE FROM FEATURES IN THE LIGHT CURVES.

From the initial inspection of the light curves we realized that there were apparently some signals at the bottom of a few light curves, which might be indicative of refracted light by a local atmosphere somewhere on the limb of Makemake. Because the features were seen in different sites whose chords were nearly central to Makemake, they did not seem a mere coincidence and required closer scrutiny.

We inspected the residuals of a square well fit to the occultation light curve of the S. Pedro de Atacama 0.5m telescope. There is a brightness increase near 5,760s UT, at about the middle of the occultation, when a central flash would be expected. The significance level of this potential spike is 3.1σ, but because the statistics are usually not Gaussian we do not consider this a firm detection.

In Fig. S3 we show the residuals of a square-well fit to the occultation light curve from Pico dos Dias. In this case there is a clear brightening event that also takes place at the middle of the occultation phase and is well above the noise, at a safe 4.8σ significance level. But contrary to the S. Pedro de Atacama 0.5m telescope data, the event takes place in a single image. Visual inspection of the image revealed a bright single pixel slightly away from the core of the point spread function, which raises the suspicion that this might be a cosmic ray hit or a single pixel event of some sort in the detector. If the flux from this pixel is removed from the total flux computation, the light curve spike disappears. Nevertheless we computed the likelihood of such an event by searching for similar single pixel events of the required brightness in the image sequence. It turns out that there were only 24 events with a similar flux level (within 20%) or higher than the alleged single pixel event, in 200 images. We computed the likelihood that such an event took place within a 4x4-pixel box (which would contain Makemake) at the precise image in the middle of the occultation. Given that the images were 50x72 pixels in size, the probability would be only 0.05%. There are alternative explanations to a cosmic ray hit: Because there was image shift of a few pixels in previous images (due to wind, telescope jitter or seeing), this could have also occurred during the acquisition of the image. Hence a very brief central flash while the telescope was shaking might have produced a point source displaced from the core of the point spread function and no smearing of the stars. This seems feasible because the pixel scale was very coarse (1.98 arcsec/pixel), but this would require a very brief and intense central flash (much shorter than the integration time). The seeing in the 5-s images was typically 2 to 2.5 arcsecs (full width at half maximum).

a)

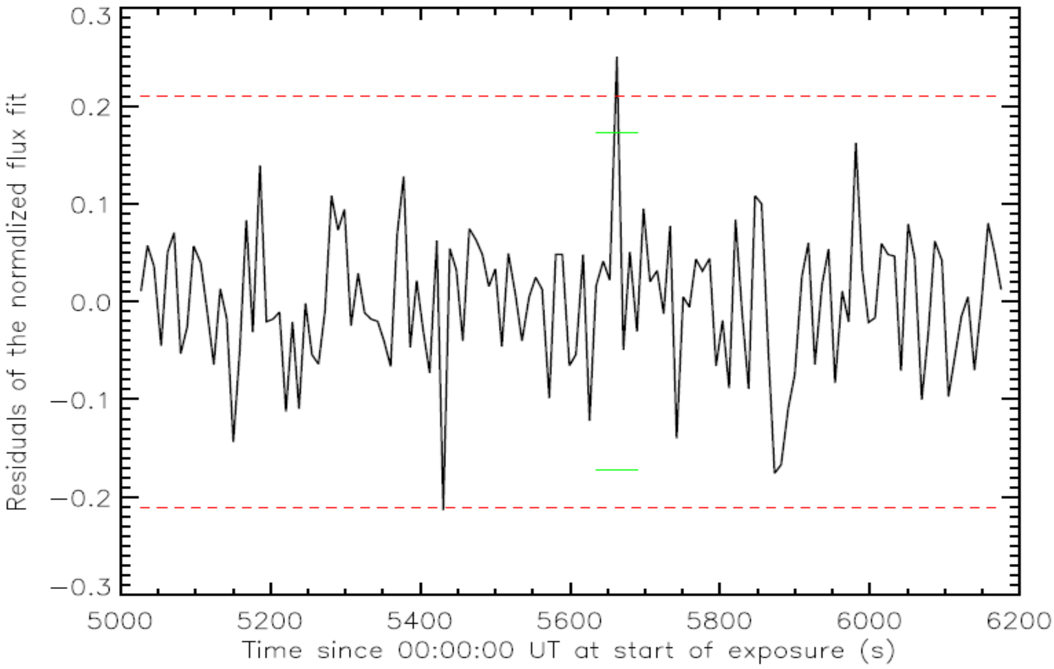

b)

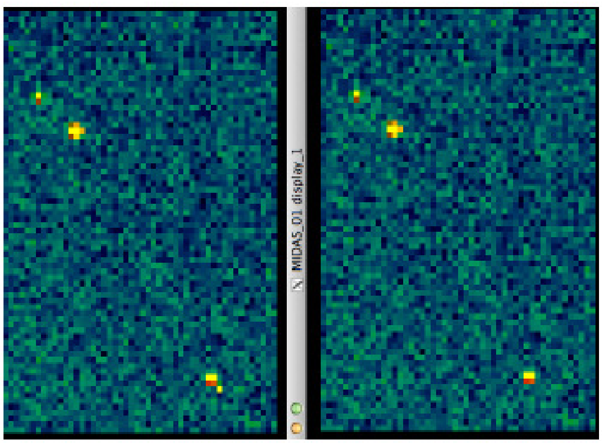

Fig. S3. a) Black solid line: Residuals of a square well fit to the Pico dos Dias occultation light curve. The brightening at around 5,660s after 0 UT is a potential central flash as it takes place in the middle of the occultation time. The brightness increase is well above the noise. By far, there is no comparable brightening in the whole observing sequence. However, this may have been produced by a cosmic ray or an image artifact (see text). The red dashed lines mark the 3σ noise levels of the light curve outside the occultation. The green solid segments represent the expected 3σ noise levels at the occultation. b) Left image: CCD image (in false color) at the time of the brightening event. The plate scale is 1.98 arcsec/pixel. Makemake is in the lower right part of the image. There is an apparent cosmic ray or image artifact close to the core of the point spread function, but slightly separated from it. The image size is 50x72 pixels. Right panel: Same as left image but with the potential artifact removed by interpolation.

In addition to the above results there is also a very marginal indication that light refracted somewhere on the limb might have reached the detector at Paranal, because there is a slight departure from a flat bottom of the curve. However, this feature in the light curve is not significant enough. It is at just 1.8 σ.

Regardless of whether the features discussed are significant or not, local atmospheres are plausible in TNOs[7], especially in Makemake, given that it has a fraction of its surface covered with a dark terrain[5,6,23] where high enough temperatures are reached and can sustain at least sublimation driven local atmospheres. Hence it makes sense to explore what kind of a local atmosphere would be consistent with the data and to see what limits we can put on such a local atmosphere.

7.1 MODELLING OF THE REFRACTED LIGHT FROM A LOCAL ATMOSPHERE

We considered a pure CH_4 atmosphere localized above patches of warmer methane ice, assuming that the subsolar point temperature reaches 50-55 K as discussed in section 5. A sketch of the location of a possible local atmosphere is show in Fig. S4. Note this is an example of a localized atmosphere, and that other configurations with other orientations and shapes could be examined. The aim of this model is to show that our data are compatible with the existence of a local atmosphere, in spite of the non-detection of a global one.

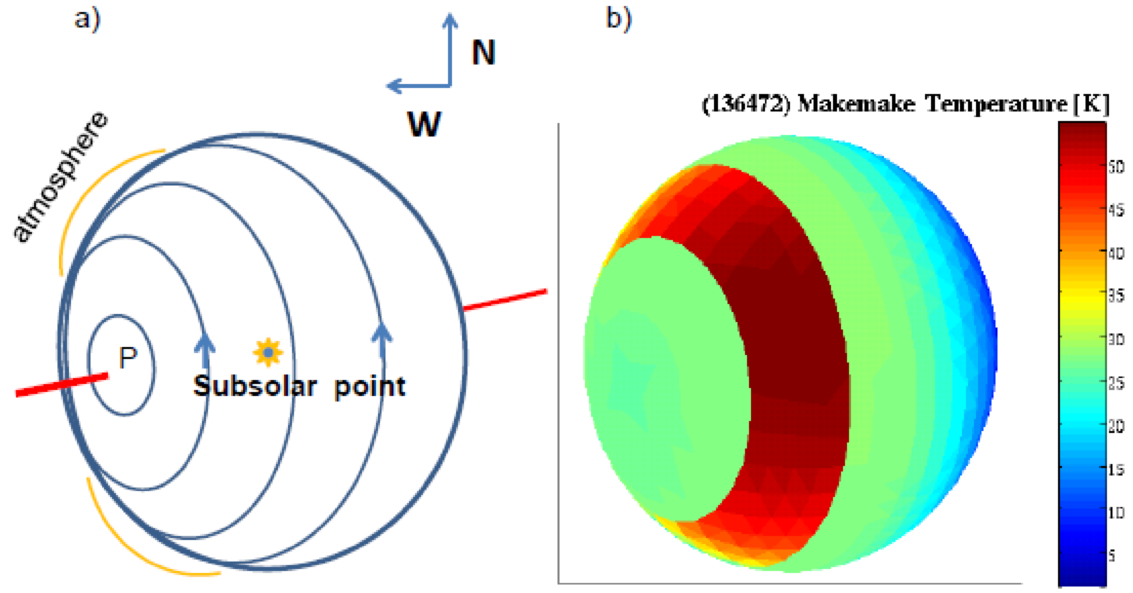

Fig. S4. a) Sketch of where a local atmosphere could roughly reside in Makemake's limb while remaining undetected at the ingresses and egresses of our light curves. A similar configuration with both the local atmosphere and the pole in the East would be valid too. The arrows indicate the assumed direction of rotation of the body and P indicates where the pole might approximately be. In this sketch an atmosphere is formed at the subsolar point and extends to the limb where it can refract light and cause effects in the occultation light curves. The atmosphere would collapse at higher latitudes and might also collapse in the night side where the temperatures are too low to maintain a sublimation driven atmosphere of a few microbar. Such an atmosphere might have a meridional flow to the poles, where the volatiles can condense and form large fresh ice caps of very high albedo. The low albedo terrain is confined to a longitudinal band near the latitude of the subsolar point. b) Thermal map of Makemake based on a thermophysical model[23].

Assuming this model, since the ingresses and egresses in all the light curves sampled areas of the body that were close to its poles, where the atmosphere should be almost collapsed (because of the considerably lower surface temperatures there, which would prevent ice sublimation), no atmosphere would be detected in the ingresses and egresses of our light curves, but a partial atmosphere could exist near the subsolar latitude and extend to the limb away from the extremities of the occultation chords (see Fig. S4). Two slightly different shapes for Makemake were used, one to explain the light curves under the assumption that the spike in the centre of the Pico dos Dias lightcurve is an artifact (and is removed from the light curve), and the other shape can explain the Pico dos Dias original light curve, assuming that the flash is real. The shapes are illustrated in Fig. S5. Both shapes fit the occultation chords. The shape in the right panel provides a slightly lower goodness of fit, but not significant from a statistical point of view.

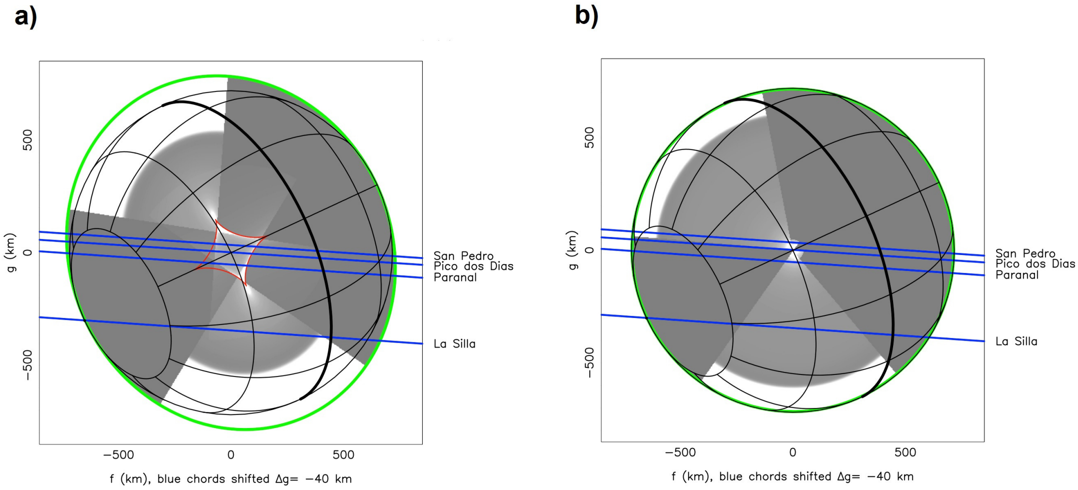

Fig. S5: a) Ray-tracing with a partial CH_4 atmosphere in the limb between 285° and 350° of Position Angle (PA), and between the symmetrical angles with respect to the minor axis (a proxy for the rotation axis). The semi-major and semi-minor axes lengths are 800 and 714 km, respectively. b) Idem, but with PAs between 275° and 350° (plus symmetrical angles), and 717 and 714 km of semi-major and semi-minor axes lengths, respectively. Both models use a temperature profile of 3 K/km until 100K is reached beyond which the atmosphere is isothermal. The surface pressure and temperature are 5 μbar and 50K. The gray scale represents the light intensity. The blue lines mark the chords at the sites indicated with labels, and the green lines indicate the local curvature of the atmosphere. The red line in the left panel marks the centers of curvature of the limb, where caustics are expected due to ray focusing. These models are used only for illustration. The modeled occultation light curves for the left and right cases are shown in Fig. S6 and compared with the observations.

In the first example (Fig. S5a) Makemake's apparent limb has semi-major and semi-minor axes of 800 km and 714 km respectively, with the semi-minor axis at position angle (PA) of 65° (measured from North and in clockwise sense). This particular shape is taken to create a curvature of the isopycnic (iso-density) atmospheric layers that causes the appropriate caustics near the shadow centre. In fact, what is important for the caustics is the curvature of the isopycnic layers. This curvature is likely to be quite different from that of the limb in the presence of a partial atmosphere. This model is not intended to fit the occultation light curves and it is used only for illustration to see whether the features it produces would be at the noise levels of the light curves.

It is also assumed that Makemake's subsolar latitude is ~30°. In that configuration, a local CH_4 atmosphere could be maintained at the subsolar point, with surface pressure P_{surf} = 3-25 μbar, corresponding to the equilibrium vapour pressure of CH_4 ice at 50-55 K and then extend to the limb.

We consider this partial atmosphere located between PA's 285° and 350° along the limb (surrounding the subsolar latitude of 30°), and we used a ray-tracing code to generate fluxes in the shadow (Fig. S5a). We adopt a temperature profile starting from 50 K at the surface with a gradient of 3 K/km, ramping up to 100 K. The main result is that a P_{surf} = 5 µbar CH_4 atmosphere (corresponding to an ice temperature of 51 K) is able to cause some bumps in the light curves at Paranal, Pico dos Dias and San Pedro de Atacama.

Note that we use a Pico dos Dias light curve corrected for the potential cosmic ray that might have occurred during the occultation. The effect at Paranal is rather modest. One can increase P_{surf} to 25 µbar to get a larger central bump at Paranal (corresponding to a CH_4 ice temperature of 55 K). In this case, the expected peaks at S. Pedro and Pico dos Dias are too big.

We have also investigated the possibility of an N_2 atmosphere at the same location along the limb as the CH_4 atmosphere considered above, with a surface temperature of 38 K, corresponding to P_{surf} = 30 µbar, ramping up like in Pluto to 100 K. It provides a central flash comparable in amplitude with the noise level in the Paranal light curve, but then provides too large flashes at S. Pedro and Pico dos Dias. Conversely, an N_2 atmosphere with P_{surf} <10 µbar would cause bumps small enough to be hidden in the noise level.

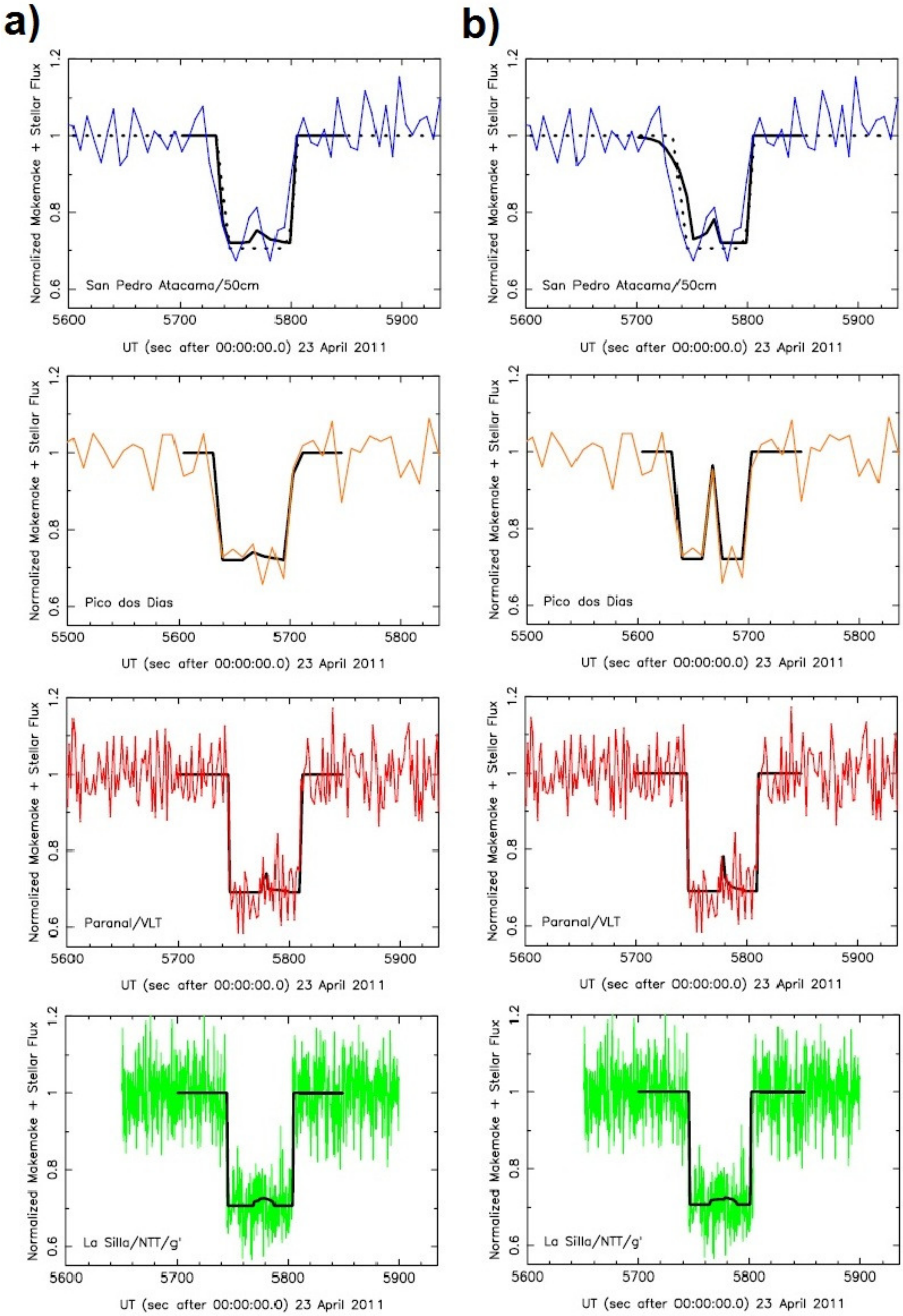
a)
b)
San Pedro Atacama/50cm
Pico dos Dias
Paranal/VLT
La Silla/NTT/g'
Normalized Makemake + Stellar Flux
UT (sec after 00:00:00.0) 23 April 2011

Fig. S6: a) Expected fluxes (black line) at S. Pedro, Pico dos Dias, Paranal and La Silla for a surface pressure P_{surf} ~5μbar using the model in the left panel of Fig. S5. (The Armazones data have not been considered here as the corresponding chord is very close to Paranal, but with a much coarser time resolution, see Fig. 1.) The fluxes from the model have been binned to the time resolution of the observed light curves (blue, brown, red, and green curves). Note that in the Pico dos Dias light curve (brown) the alleged cosmic ray has been removed. The χ^2 values of the fits were 36.2, 13.2, 91.7 and 738.3 for 25, 17, 99, and 540 data points respectively. Thus, the square root of χ^2/N is close to 1 in all cases, indicating that the fits are reasonably good. However, these models are just for illustration. b) Same as panels a, but with the shape model in the right panel of Fig. S5 (note this model can explain a central flash at Pico dos Dias). Note that the Pico dos Dias light curve (brown) is shown as it was initially obtained, with no removal of a potential cosmic ray. The χ^2 values of the fits were 43.3, 22.6, 88.1 and 794.1. The dotted line in the S. Pedro panels is the expected light curve from an airless body.

In the second example, a less elongated Makemake's atmosphere has been used (Fig. S5b). The differences with the other model are the dimensions of the body (1,428 km and 1,434 km for the projected minor and major axes) and the position angles (275° to 350°) for the local atmosphere. The synthetic light curves from the local CH_4 atmosphere are plotted in the right panels of Fig. S6. This model reproduces a flash at Pico dos Dias while preserving the fluxes at S. Pedro and Paranal low. Similar models but with elongations up to 1.06 can give rise to a flash in Pico dos Dias while creating small signals at S. Pedro and Paranal.

We point out that the models presented here depend on several parameters that we do not know. Exploring the possible phase space is clearly out of the scope of this work. This said, the main lesson learnt from our modelling is that a patchy CH_4 or N_2 atmosphere with P_{surf} of a few μbar may be present in the upper and lower left quadrants of the limb and cause structures compatible with the observed light curves. Larger surface pressures would cause too intense features.

8. PREFERRED PROJECTED SHAPE, ASPECT ANGLE AND DENSITY FOR MAKEMAKE.

The elongation direction in the best ellipse fit shown in the main paper is almost perpendicular to the chords direction (Fig. 2). This seems too coincidental. In reality, the elongation in that direction is probably an artificial result because the length of the axis in the direction perpendicular to the chords is not well constrained by the observations. This is usually the case for a nearly spherical body when there are no negative chords sufficiently separated from the positive chords. The same effect was also seen in the occultation by Eris[3], for which a large set of ellipse solutions was possible with considerable elongation in the direction perpendicular to the chords. Thus, we think that the elongation of the nominal best ellipse fit for Makemake in Fig. 2 is too large to be real and is mainly a result of limitations in the observations, similarly to the case of Eris.

We know that the purely circular fit is also unlikely because the general projection of a Maclaurin spheroid is an ellipse and only the pure pole-on orientation can give rise to a circle (but a pure pole-on configuration is very unlikely).

On the other hand, the low rotational variability of Makemake[28,20,21] can be explained if the object has a very homogeneous surface with perhaps a latitudinal band, or if its spin axis orientation is not too far from pole-on. Probably the reality is a mix of the two causes (which we show in Fig. S4). Because the object must have a Maclaurin shape as explained in the main paper, and the projection of a Maclaurin seen far from the equator-on view is closer to a circle than to a very elongated shape, the low rotational variability would favor a fit closer to the circular one than to the very elongated nominal ellipse fit (which has an axial ratio of 1.15).

Besides, the comparison of the Spitzer+Herschel data with the occultation favors the smaller object, which is the nearly circular fit, because the nominal elliptical solution with an axial ratio of 1.15 implies a larger body than is compatible with the Spitzer+Herschel results at almost 2σ. The equivalent diameter of the ellipse with an axial ratio of 1.15 is 1,533 km, away from the maximum diameter allowed for by Spitzer+Herschel (ref. 6).

As mentioned in the main paper, for a spherical Makemake of 1,430 km diameter, a density of ~1.7 g/cm^3 is derived to explain the lack of a global atmosphere, using volatile loss models[8]. In this case the body would not have had enough mass to retain the primordial N_2. The derived 1.7 g/cm^3 density is consistent with the trend observed empirically, as can be seen in Fig. S7. But if Makemake had a projected axial ratio as large as 1.15 (the nominal ellipse fit), the equivalent diameter would be 1,533 km and Makemake would require a smaller density than 1.5 g/cm^3 to be depleted in N_2, according to the volatile loss models[8]. Such a low density for a larger object would be further away from the trend of density versus size than the 1.7 g/cm^3 value (see Fig. S7). Thus, these considerations also indicate that the circular model (the smaller object) is slightly preferred with respect to the nominal ellipse fit. Nevertheless if the lack of a global atmosphere on Makemake is not a result of a surface depletion in N_2 but to a pole-on orientation, this is again in favour that Makemake's projected shape is closer to circular rather than having a 1.15 axial ratio. According to section 6.2 of a theoretical study on TNO atmospheres[7], TNOs with orientation close to pole-on are less likely to develop global atmospheres.

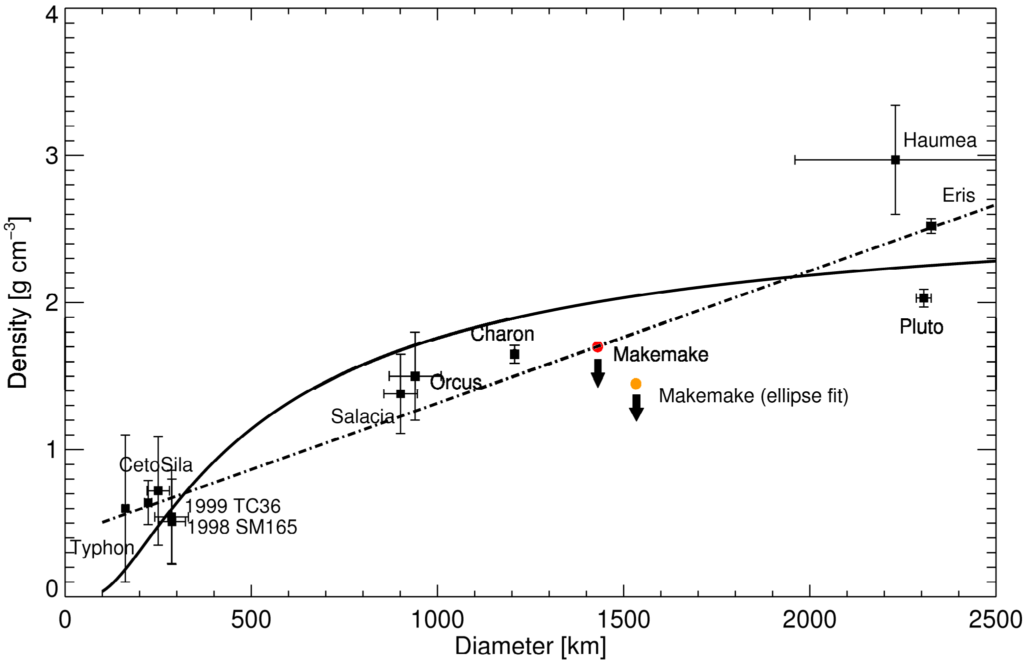

Fig. S7: Plot of density versus diameter for TNOs from a compilation of different sources of data[3,19,33,34,35,36,37,38,39,40]. Two density estimates for Makemake from this paper are shown in red and yellow. The red spot value was obtained by assuming that Makemake is depleted in N_2 ice and using the model in ref. 8 to determine the density below which N_2 would not be retained (using the size determined from the circular fit to the occultation chords). The yellow dot is the same as the red one but using the size derived from the best ellipse fit in Fig. 2 of the main paper, which required an axial ratio of 1.15 and implied a larger body. In reality, the dots indicate upper limits because lower densities also result in no N_2 retention. On the other hand, because methane is retained in Makemake (it is clearly seen in its spectra), the densities must be higher than 1.4 and 1.2 g/cm^3 for the red and yellow dots (using again the model in ref. 8, but this time for methane). This is marked by the arrows. The yellow spot is far from the observed trend and appears less likely. The dashed line is a linear fit to the data, and the continuous line is an exponential fit.

A Maclaurin spheroid of 1.7 g/cm^3 density, spinning at 7.77 hours, would have a true (not projected) axial ratio of 1.17 according to the figures of equilibrium formalism, but when viewed with an aspect angle of 35 degrees (a reasonable angle according to the above discussions) the object would give a projected axial ratio of 1.05. A maximum aspect angle of 45 degrees (corresponding to an orientation exactly in the middle between pole-on and equator-on) would give rise to a projected axial ratio of slightly less than 1.08.

Also, the model of a possible central flash in Pico dos Dias, described in section 7, requires a limb less elongated than 1.06 (in axial ratio) including the atmosphere. Then, if the flash is real, the object would have to be even less elongated than 1.06 in projected axial ratio.

In summary, there are six different indications to favor the solution between the circular model and the nominal ellipse fit: The degeneracy in the direction perpendicular to the chords, the low rotational variability, the fact that for a plausible aspect angle and a plausible density the projected axial ratio would be close to 1.05 (for a body rotating at 7.77h), the lack of a global atmosphere, the comparison with Spitzer+Herschel data, and the possible central flash. These indications point to a projected shape between the circular model and the best ellipse fit, although closer to the circle. The best compromise is for a projected axial ratio of 1.05 ± 0.03. For all the above, the preferred solution from the occultation of Makemake is an ellipse with minor axis 1,430±9 km and major axis 1,502±45 km. Concerning the preferred density, even though the volatile retention arguments point to a density of 1.7 g/cm^3, the models of volatile loss and retention are too simplistic to account for all the processes, and therefore this result is only approximate (but consistent with the value derived from the density vs size trend shown in Fig. S7). A possible indication of the accuracy of this value may be obtained from the dispersion in Fig. S7. Because the dispersion is on the order of 0.3 g/cm^3, we can state that the density of Makemake should probably range from 1.4 to 2.0 g/cm^3.

REFERENCES

28. Ortiz, J. L. *et al.* A mid-term astrometric and photometric study of trans-Neptunian object (90482) Orcus. Astron. Astrophys. 525, id. A31 (2011)

29. Brucker *et al.* High albedos of low inclination Classical Kuiper belt objects. Icarus 201, 284-294 (2009)

30. Lellouch, E. *et al.* Pluto's Non-isothermal Surface. Icarus 147, 220-250 (2000)

31. Lellouch, E. The thermal structure of Pluto's atmosphere: clear vs hazy models. Icarus 108, 255-264 (1994)

32. Strobel D.F. and Zhu X. On the Vertical Thermal Structure of Pluto's Atmosphere. Icarus 120, 266-289 (1996)

33. Grundy, W. M. *et al.* Mutual events in the Cold Classical transneptunian binary system Sila and Nunam. Icarus 220, 74-83 (2012)

34. Stansberry, J. A. *et al.* Physical properties of trans-neptunian binaries (120347) Salacia-Actaea and (42355) Typhon-Echidna. Icarus 219, 676-688 (2012)

35. Santos-Sanz, P. *et al.* "TNOs are Cool": A survey of the trans-Neptunian region. IV. Size/albedo characterization of 15 scattered disk and detached objects observed with Herschel-PACS. Astron. Astrophys. 541, id. A92 (2012)

36. Vilenius, E. *et al.* “TNOs are Cool": A survey of the trans-Neptunian region. VI. Herschel/PACS observations and thermal modeling of 19 classical Kuiper belt objects. Astron. Astrophys. 541, id. A94 (2012)

37. Buie, M. W., *et al.* Orbits and Photometry of Pluto's Satellites: Charon, S/2005 P1, and S/2005 P2. Astron. J. 132, 290-298 (2006)

38. Benecchi, S. D., et al. (47171) 1999 TC_{36}, a transneptunian triple. Icarus 207, 978-991(2010)

39. Spencer, J. R. *et al.* A Low Density for Binary Kuiper Belt Object (26308) 1998 SM_{165}. Bull. Amer. Astron. Soc., 38, 546-546 (2006)

40. Brown, M. E. *et al.* The Size, Density, and Formation of the Orcus-Vanth System in the Kuiper Belt. Astron. J. 139, 2700-2705 (2010)